Hydrol. Earth Syst. Sci. Discuss., 7, 649–686, 2010
www.hydrol-earth-syst-sci-discuss.net/7/649/2010/

Hydrology and Earth System Sciences Discussions

This discussion paper is/has been under review for the journal Hydrology and Earth System Sciences (HESS). Please refer to the corresponding final paper in HESS if available.

Modelling soil moisture at SMOS scale by use of a SVAT model over the Valencia Anchor Station

S. Juglea[1], Y. Kerr[1], A. Mialon[1], J.-P. Wigneron[2], E. Lopez-Baeza[3], A. Cano[3], A. Albitar[1], C. Millan-Scheiding[3,4], M. Carmen Antolin[4], and S. Delwart[5]

[1]Centre d'Études Spatiales de la BIOsphère, UMR 5126 (CNRS, CNES, IRD, UPS), Toulouse, France
[2]Ecologie fonctionnelle et PHYSique de l'Environnement (INRA/EPHYSE), Bordeaux, France
[3]Universitat de Valencia, Departament de Termodinamica i Fisica de la Terra, Valencia, Spain
[4]Center for Desertification Research (CIDE), Dept. of Territorial Planning, Valencia, Spain
[5]European Space Research and Technology Centre (ESA/ESTEC), Noordwijk, The Netherlands

Received: 21 December 2009 – Accepted: 23 December 2009 – Published: 27 January 2010

Correspondence to: S. Juglea (silvia.juglea@cesbio.cnes.fr)

Published by Copernicus Publications on behalf of the European Geosciences Union.

Abstract

The main goal of the SMOS (Soil Moisture and Ocean Salinity) mission is to deliver global fields of surface soil moisture and sea surface salinity using L-band (1.4 GHz) radiometry. Within the context of the preparation for this mission over land, the Valencia Anchor Station experimental site, in Spain, was chosen to be one of the main test sites in Europe for the SMOS Calibration/Validation (Cal/Val) activities. Ground and meteorological measurements over the area are used as the input of a Soil-Vegetation-Atmosphere-Transfer (SVAT) model, SURFEX (Externalized Surface)-module ISBA (Interactions between Soil-Biosphere-Atmosphere) so as to simulate the surface soil moisture. The calibration as well as the validation of the ISBA model was made using in situ soil moisture measurements. It is shown that a good consistency was reached when point comparisons between simulated and in situ soil moisture measurements were made. In order to obtain an accurate soil moisture mapping over the Valencia Anchor Station ($50\times50\,km^2$ area), a spatialization method has been applied. To validate the approach, a comparison with remote sensing data from the Advanced Microwave Scanning Radiometer on Earth observing System (AMSR-E) and from the European Remote Sensing Satellites (ERS-Scat) was performed. Despite the fact that AMSR-E surface soil moisture product is not reproducing accurately the absolute values, it provides trustworthy information on surface soil moisture temporal variability. However, during the vegetation growing season the signal is perturbed. By using the polarization ratio a better agreement is obtained. ERS-Scat soil moisture products were also used to be compared with the simulated spatialized soil moisture. The seasonal variations were well reproduced. However, the lack of soil moisture data over the area (45 observations for one year) was a limit into completely understanding the soil moisture variability.

1 Introduction

Soil moisture is a key variable controlling the exchanges of water and energy at the surface/atmosphere interface (Betts et al., 1996; Entekhabi et al., 1996). It is highly variable both spatially and temporally as the result of the spatial heterogeneity of soil and vegetation properties, topography, land cover, rainfall and evapo-transpiration (Bosch et al., 2006; Entekhabi and Rodrigues-Iturbe, 1994). Observing the spatial distribution of soil moisture at the catchement scale is a difficult task requiring intensive field instrumentation for accurate spatial and temporal representation. Nowadays, remote sensing technology has matured to the point that surface soil moisture can be estimated at global scale from space (Wigneron et al., 2003; Wagner et al., 2006). Microwave remote sensing at low frequencies have been found to produce the best results (Kerr, 2007; Wagner et al., 2006; Njoku and Entekhabi, 1996; Jones et al., 2004). In spite of the importance of soil moisture observations, the instruments that have been or are currently operating are not dedicated to soil moisture monitoring. However, there are a number of soil moisture products available from different sensors. The Advanced Microwave Scanning Radiometer for the Earth Observing System (AMSR-E) (Njoku et al., 2003) on board the National Aeronautics and Space Administration's (NASA) Aqua satellite and the scatterometers (Scat) on board the European Remote Sensing Satellites 1 and 2 (ERS-1 and ERS-2) (Wagner et al., 1999a) provide soil moisture products. Both instruments use frequencies above 5 GHz.

The SMOS (Soil Moisture and Ocean Salinity) (Kerr et al., 2001) mission was designed to measure soil moisture over continental surfaces as well as ocean salinity using a low microwave frequency – L-band (1.4 GHz). At this frequency, microwave observations are sensitive to soil moisture through the effects of moisture (water) on the dielectric constant and hence on the emissivity of the soil. The soil emission is integrated over a soil depth of a few centimeters, giving a more representative measurement of soil moisture conditions over this layer. Consequently, SMOS should be able to derive soil moisture with better than 0.04 m^3/m^3 accuracy (Kerr et al., 2001). The

passive microwave observations are done at multiple viewing angles between 0°and 55°, and with a spatial resolution ranging from 35 km at nadir up to 50 km (Kerr et al., 2001). Launched in November 2009, SMOS is the first mission dedicated to surface soil moisture measurement and will provide global soil moisture maps twice (06:00 a.m. and 06:00 p.m.) a day in less than 3 days. L-band passive microwave radiometry is a very useful tool for soil moisture monitoring, allowing nearly all weather observation, surface vegetation cover information and surface brightness temperature. Numerous field experiments using ground based and airborne L-band observations indicated a soil moisture retrieval capability of better than 0.04 m^3/m^3 accuracy (Wang et al., 1990a; Schmugge et al., 1992; Jackson et al., 1995, 1999). In this context, the strategy adapted by ESA for its Soil Moisture and Ocean Salinity mission was to develop specific land product validation activities over well equipped monitoring sites. The Valencia Anchor Station (Lopez-Baeza et al., 2005a,b), in eastern Spain, and the Upper Danube Catchment (Delwart et al., 2007), in southern Germany, are chosen as the two main test sites in Europe for the SMOS Calibration/Validation (Cal/Val) activities. This article will focus over the Valencia Anchor Station site which is a large reference area, sufficiently equipped with ground soil moisture probes and fully characterized so as to contribute to SMOS land product validation. In the framework of SMOS preparation, the aim of this study is to give a first insight into the SMOS data by generating a spatialized surface soil moisture over an area of 50×50 km^2 (equivalent with a SMOS pixel). To perform this, surface variables (ground and meteorological measurements) from the Valencia Anchor Station are used as inputs to the Soil-Vegetation-Atmosphere-Transfer (SVAT) model (ISBA) (Noilhan and Planton, 1989; Noilhan and Mahfouf, 1996) from Météo-France. The accuracy of the approach was tested by comparing its results with data products derived from AMSR-E and ERS-Scat.

2 Valencia Anchor Station – experimental domain and data

The Valencia Anchor Station (VAS) site was established in December 2001 (Lopez-Baeza et al., 2002) by the University of Valencia (see http://www.uv.es/anchors and http://www.uv.es/elopez) with the main objective of characterizing a large-scale reference Cal/Val area specifically dedicated to the validation of low spatial resolution Earth Observation data products. It is located in Spain close to the town of Caudete de las Fuentes (39°33′32″ N, 1°16′37″ W), at about 80 km West of the city of Valencia.

2.1 Characteristics of the area

The Valencia Anchor Station test site represents a reasonably homogeneous and flat area of about 50×50 km^2 (Fig. 1). The main cover type is vineyards, about 56%, followed by trees, shrubs, forest, industrial and urban. Beside the vineyard growing season, the area remains mostly under bare soil conditions. In spite of its relatively flat topography, the small altitude variations of the region clearly influence climate. It oscillates between semiarid in the areas of the towns of Utiel and Caudete de las Fuentes and dry-sub-humid towards Villagordo del Cabriel (about 16 km from Caudete de las Fuentes). The altitudinal differentiation between both climate types corresponds to levels 800–850 m a.s.l. Annual mean temperatures oscillate between 12 °C at Villagordo del Cabriel and 14.2 °C at Caudete de las Fuentes. Annual precipitation varies between 396 mm in Utiel and 451 mm of Caudete de las Fuentes and Villagordo del Cabriel. The duration of frost free periods is similar for the three town areas, from May to November. Maximum precipitations occur in spring and autumn. The spring maximum is generally in May, whereas the autumn maximum is variable, in October for Caudete de las Fuentes and Utiel, and November for Villagordo del Cabriel.

2.2 Available data over the area

The methodology of this article is to produce spatially distributed and validated soil moisture maps over the VAS 50×50 km^2 area. For this purpose, in situ measurements and remotely sensed data products were used. The characteristics of these data are depicted next.

2.2.1 In situ measurements

Valencia Anchor Station is characterized by an extensive set of measurements at different levels (in the atmosphere and in the soil) in order to derive surface energy fluxes. Over the 50×50 km^2 area 22 meteorological stations are available (Table 1), 4 fully equipped and 18 rain gauges are not uniformly distributed (Fig. 2). The 4 fully equipped stations measure meteorological data: air temperature and humidity at screen level, atmospheric pressure, precipitation, wind speed and direction and solar and atmospheric radiation. The topography is mostly flat and soil use is well differentiated between vineyards, almond, olive, pine-trees and shrubs. In the VAS area the soil texture is a parameter that depends mainly on lithology (Lopez-Baeza et al., 2008). So as to have an accurate spatial distribution of the texture, a map of clay and sand (Millan-Scheiding et al., 2008) at 10 m resolution covering all the 50×50 km^2 area was used. Leaf area index (LAI), roughness and fraction of vegetation were measured during short time periods. However, the period considered in this article is from 2005 to 2007. Remote sensed LAI data was used (see Sect. 2.2.2.). The historical data for the roughness and the fraction of vegetation was obtained from ECOCLIMAP, a global land use maps database at 1 km resolution (Masson et al., 2003). Over the 50×50 km^2 area two major ground measurement campaigns took place.

The first campaign, called Melbex I (Cano et al., 2009) (Mediterranean Ecosystem L-Band characterization Experiment), was carried out between June 2005 and January 2006 to observe the surface emission of Mediterranean shrubs. The soil was characterized as sandy, with a soil texture composed of 47% sand, 38% of silt and 15% clay.

HESSD
7, 649–686, 2010

The vegetation is well adapted to dry conditions in summer and to freeze conditions in winter. The vegetation biomass is only subject to small variations throughout the year, it does not generally grow over a meter high and its distribution is random. Soil moisture measurements were carried out for the top first 5 cm of the soil, at 12 points every 10 min using capacitive probes. The ground soil moisture measurements were randomly scattered over the study area by placing probes both over bare soil and under shrubs. The probes were calibrated under laboratory conditions at the end of the experiment using the same soil type in order to correctly convert the raw voltage values into volumetric soil moisture content (m^3/m^3).

The second soil campaign, Melbex II (Cano et al., 2008) (Mediterranean Ecosystem L-Band characterization Experiment), was carried out from April 2007 to December 2007 to observe the surface emission of vineyards. The soil is characterized as sandy clay loam, with a texture composed of 45% sand, 29% of silt and 26% clay. As in the previous experiment, soil moisture measurements were carried out at different representative points every 10 min using the same capacitive probes. In the area, the soil was ploughed at least 3 times during the growing period of vineyards.

2.2.2 Remote sensing data

Satellites data are used in this article. A short description of each of these data is given below.

– AMSR-E data

The Advanced Microwave Scanning Radiometer (AMSR) of the Earth Observing System (EOS) is a multi-channel passive microwave instrument, launched on the Aqua satellite in May 2002. It operates in polar sun-synchronous orbit with equator crossing at 01:30 p.m. and 01:30 a.m. local solar time. Global coverage is achieved every two days or less depending on the latitude. The AMSR-E instrument measures dual polarized radiation at six frequencies in the range of 6.9 to 89 GHz, with an incidence angle of 55°. The mean spatial resolution at 6.9 GHz is about 56 km with a swath width of

1445 km. In order to minimize the atmospheric effects and to maximize vegetation and soil penetration, the inversion algorithm for the retrieval of soil moisture was designed to use the C-band frequency in preference to the higher ones. However, due to the high level of RFI observed by AMSR-E at 6.9 GHz, the current AMSR-E soil moisture retrievals use only the 10.7 GHz and higher frequencies (Njoku et al., 2003).

The data used in this study are from the National Snow and Ice Data Center (NSIDC) Level 3 AMSR-E dataset (Njoku, 2004). The daily averages of brightness temperature and soil moisture products are re-sampled to a global cylindrical 25 km Equal-Area Scalable Earth Grid (EASE-Grid) cell spacing (Njoku, 2004). Two AMSR-E soil moisture sampled pixel are covering the VAS area. The average of these two pixels was considered to be representative for the $50 \times 50\,km^2$ area. In addition to the soil moisture, the polarization ratio (PR) at 6.9 Ghz is used and is defind as:

$$PR = \frac{Tb_v - Tb_h}{Tb_v + Tb_h} \quad (1)$$

It normalize out the surface temperature and leave a quantity that depends primarily on soil moisture, vegetation and atmosphere (Kerr and Njoku, 1990; Njoku et al., 2003; Owe et al., 2001). At low microwave frequencies, the polarization ratio has often been used to study soil moisture and vegetation effects. Its dynamic is well related to the soil moisture variations. At increasingly large angles (55° in this case) there is a longer observation path through the vegetation layer, causing greater attenuation of the emission from the underlying soil and reducing the sensitivity to the soil moisture (Njoku et al., 2003). Several studies investigated the validation and evaluation of AMSR-E soil moisture product (Gruhier et al., 2008; Rüdiger et al., 2009). As the AMSR-E soil moisture product shows biases and very small amplitude, a normalization between [0, 1] was done using:

$$y' = \frac{y - y_{min}}{y_{max} - y_{min}} \quad (2)$$

where y' is the normalized curve and y is the input curve (in this case y is considered as the soil moisture product). Consequently, the discussion of this paper will focus on the normalized dataset.

– ERS-SCAT data

The ERS (European Remote Sensing Satellites) scatterometer is an active low-resolution microwave sensor flown on the board of the ERS-1 and ERS-2 satellites. ERS-1 was launched in July 1991 followed by the identical ERS-2 in 1995. The first objective of this sensor is to measure wind over oceans, but its measurements have been shown to be highly suitable for surface soil moisture remote sensing (Magagi and Kerr, 1997; Wagner et al., 1999a). The ERS scatterometer operates at 5.3 GHz (C-band), vertical polarization, collecting backscatter measurements over an incidence angle range from 18° to 57°. It operates in polar sun-synchronous orbit with equator crossing times at 10:30/22:30. The spatial resolution of the ERS-Scat footprint is about 50 km with a 12.5 km spatial sampling interval, giving 16 ERS-Scat soil moisture products over the $50 \times 50\,km^2$ area. In order to have a maximum temporal and spatial cover, the mean value of the 16 pixels was considered to be representative over the VAS area. The surface soil moisture data are retrieved from the radar backscattering coefficients, using the change detection method suggested by Dobson and Ulaby (1976). The methodology is described by Wagner et al. (1999a,b) which exploits the information provided by the multiple incidence angle measurements acquired by the ERS scatterometer. Knowing the incidence angle dependency, the backscattering coefficients are normalized to a reference incidence angle of 40°. The relative soil moisture data ranging from 0% to 100% are derived by scaling the normalized backscattering coefficients between the lowest/highest values corresponding to the driest/wettest soil conditions.

– MODIS

The Moderate Resolution Imaging Spectroradiometer (MODIS; http://modis.gsfc.nasa.gov/) is an instrument on board of NASA's Terra and Aqua platforms. The MODIS LAI

(Leaf Area Index) product is globally tiled and is projected on a sinusoidal grid which is an equivalent projection conserving the surface areas. They are at 1 km spatial resolution provided on a daily and 8-day basis and there are used as input to the SVAT model.

– METEOSAT

In order to run the SVAT model and so to produce soil moisture maps, an atmospheric forcing is needed. One of the parameters of the atmospheric forcing is the shortwave radiation. As already mentioned, over the area only 4 meteorological stations measuring shortwave radiation are available. For a better resolution over the entire area, the shortwave values were derived from Meteosat. The instrument is a geostationary weather satellite launched by the European Space Agency (ESA). The Meteosat radiometer is an instrument sensitive to visible and thermal radiation.

The SVAT model is used to generate, from atmospheric forcing and initial conditions, the temporal behavior of the soil moisture. Spatialy distributed fields and forcing enables to simulate soil moisture spatial and temporal behavior and thus averaged soil moisture at any moment for the whole pixel ($50 \times 50\,km^2$). The model used is called SURFEX (stands for surface externalisée – Le Moigne et al., 2009) and was developed at the National Center for Meteorological Research (CNRM) at Météo-France. It gathers all the developments and improvements made in surface schemes, containing four different modules: ISBA (Interactions between Soil-Biosphere-Atmospherefor), Sea and ocean, TEB (Town Energy Balance) and Lake. In this article only the module for the soil and vegetation – ISBA (Noilhan and Planton, 1989) was used. ISBA is a soil-vegetation-atmosphere transfer (SVAT) scheme which describes the exchanges of heat and water between the low-level atmosphere, the vegetation and the soil. It is a relatively simple scheme, which takes into account the most important components of the land surface processes. It depends on the type of soil and of vegetation. It has been widely validated over vegetated and bare ground surfaces (Mahfouf and Noilhan, 1991; Calvet et al., 1998). The soil module in ISBA can be run in different configurations: 2-layers, 3-layers (ISBA-2L, ISBA-3L – with force-restored discretization) and

HESSD
7, 649–686, 2010

diffusive (ISBA-DIF). New possibilities comparing with ISBA-2 or 3 layers are available by using ISBA-DIF: the computation of a vertical profile of the temperature, liquid water and ice content over as many layers as needed. This scheme has already been applied successfully over a fallow site (Boone et al., 2000) and an agricultural site (Boone et al., 1999), where in situ data collected at several depths allowed a validation of the simulation. In order to select the most appropriate configuration, different tests have been made. A significant decrease in error was obtained in the case of a diffusive scheme so for our study the ISBA-DIF model was used. The equations that governs the temporal evolution ∂t of the heat and mass transfer from the surface down through the soil column for the snow-free case (Boone et al., 2000; Boone, 2000) are written as follows:

$$c_h \frac{\partial T_g}{\partial t} = \frac{\partial G}{\partial z} - \Phi \tag{3}$$

$$\frac{\partial w_l}{\partial t} = -\frac{\partial F}{\partial z} - \frac{\Phi}{L_f \rho_w} - \frac{S_l}{\rho_w} \qquad (w_{\min} \le w_l \le w_{\text{sat}} - w_i) \tag{4}$$

$$\frac{\partial w_i}{\partial t} = \frac{\Phi}{L_f \rho_w} - \frac{S_i}{\rho_w} \qquad (0 \le w_i \le w_{\text{sat}} - w_{\min}) \tag{5}$$

where, Eq. (3) represents the vertical component of the heat transfer equation, c_h being the total heat capacity ($\mathrm{J\,m^{-3}\,K^{-1}}$), G is the soil heat flux ($W\ \mathrm{m^{-2}}$), T_g is the composite soil-vegetation temperature (K) at the surface and the soil temperature only for subsurface layers, Φ is the latent heat source/sink resulting from phase transformation of soil water and z (m) is the soil depth which is increasing downward. The Eqs. (4) and (5) represent the volumetric liquid water (w_l) and ice liquid water equivalent (w_i) contents of the soil ($\mathrm{m^3\,m^{-3}}$), respectively. They are related to the total volumetric water content (w) ($\mathrm{m^3\,m^{-3}}$) through:

$$w = w_l + w_i \tag{6}$$

S_l (evapotranspiration, lateral inflow) and S_i (sublimation) represent external sources/sinks ($kg\,m^{-3}\,s^{-1}$), of the liquid and ice liquid equivalent soil water, F is the vertical water flux due to drainage and diffusion ($m\,s^{-1}$), L_f is the latent heat of fusion ($3.337\times105\,J\,kg^{-1}$), and ρ_w is the density of liquid water ($1000\,kg\,m^3$). The total soil porosity is w_{sat} ($m^3\,m^{-3}$), and w_{min} is the minimum liquid water content ($0.001\,m^3\,m^{-3}$). The continuity equation for the total soil volumetric water content is obtained by adding (4) and (5):

$$\frac{\partial w}{\partial t} = -\frac{\partial F}{\partial z} - \frac{1}{\rho_w}(S_i + S_l) \qquad (w_{min} \le w \le w_{sat}) \tag{7}$$

Soil water transfer (infiltration, runoff, diffusion and drainage) in SVAT's is governed by equations which attempt to characterize the soil through a set of hydrological parameters. The ISBA scheme uses the Clapp and Hornberger (1978) soil water model, which is common to a large number of surface parametrization schemes. The estimation of the diffusion of water in the soil is based on Darcy's law, where the water vertical flux is proportional to the gradient of the matric potential through the hydraulic conductivity.

$$F = -k\frac{\partial}{\partial z}(\Psi + z) - D_{v\Psi}\frac{\partial \Psi}{\partial z} - K_d \tag{8}$$

where $D_{v\Psi}$ is the vapor conductivity (Braud et al., 1993), Ψ is the soil water matric potential (m) , K_d is an additional linear background drainage term ($m\,s^{-1}$) and k is the hydraulic conductivity ($m\,s^{-1}$). The hydraulic conductivity k ($m\,s^{-1}$) and the soil water matric potential Ψ (m) are related to the liquid volumetric soil water content through (Brooks and Corey, 1966; Clapp and Hornberger, 1978):

$$k = k_{sat}\left(\frac{w_l}{w_{sat}}\right)^{2b+3} \tag{9}$$

$$\Psi = \Psi_{sat}\left(\frac{w_l}{w_{sat}}\right)^{-b} \tag{10}$$

where b is the coefficient of the water retention curve.

2.3 Calibration of the SVAT model

In this section, the different sensitivity studies made as well as the parametrization chosen for the soil hydraulic functions are described.

ISBA's configuration contains 12 patches for the vegetation parametrization. For our case study, as the vegetation on our site is composed mainly by vineyards, almonds trees and shrubs, the crops case was considered.

The atmospheric forcing is used as an input of the SVAT model to obtain the surface soil moisture. The atmospheric forcing, needed to run the ISBA model, is composed of: air temperature and humidity at screen level, atmospheric pressure, precipitation, wind speed and direction and solar and atmospheric radiation. According to the dataset, these external forcing data are registered on a 30/60 min basis in the 4 fully equipped meteorological stations located into the $50 \times 50\,km^2$. Among the rain gauges, some of them are recording the weather information daily. In order to run the SVAT models with a suitable temporal resolution, standard diurnal cycles were reconstructed from the daily data. Another important aspect is the soil layer discretization, is to unable one to compare realistic configurations as a function of the penetration depth, between ground measurements and/or the remote sensing data. A sensitivity study was conducted in order to test the influence of different parameters. The most representative configuration was chosen with 13 layers, with different thickness, from 1 cm at the surface down to 1.50 m of depth (1, 2, 3, 4, 5, 7, 9, 10, 30, 50, 80, 100, 150 cm).

The performance of the land-surface schemes and hence the soil moisture simulations are sensitive to the choice of soil hydraulic parameters (Shao and Henderson-Sellers, 1996). Most of these hydrological parameters are site dependent. They are obtained from measurements or they are prescribed. It is difficult to prescribe a value for the wilting point (w_{wilt}), field capacity (w_{fc}), hydraulic conductivity at saturation (k_{sat}), saturated soil moisture (w_{sat}), the coefficient of the water retention curve (b) or for the matric potential at saturation (Ψ_{sat}). These parameters are nonlinearly related to soil moisture through empirical equations. So as to take into account the characteristics

of the area, the establishment of new databases for soil hydraulic parameters is necessary to improve the soil moisture simulations. The hydrological parameters of the soil (k_{sat}, w_{sat}, b, Ψ_{sat}) are calculated using empirical equations as a function of the percentages of sand and clay. Using ISBA's default relations (Giordani, 1993; Noilhan and Lacarrère, 1995) to compute the soil parameters (see Table 2), the simulated soil moisture obtained is not in perfect accordance with the ground measurements. In order to minimize this difference, a new set of equations (see Table 2) for the soil hydraulic parameters are established using Cosby et al. (1984); Boone et al. (1999). These calibrated equations were optimized inside the confidence interval defined in Cosby et al. (1984); Boone et al. (1999). Both sets of data, the one used by default ISBA and the one from the calibrated version, were obtained from the same 11 textural classes and the same dataset.

The results of the comparison between ground measurements and the simulated soil moisture using the new set of equations are given in Sect. 4.

2.4 Spatialization method

The distribution of soil moisture patterns throughout a catchment plays a critical role in a variety of hydrological processes. Observing the spatial distribution of soil moisture at the catchment scale is a difficult task requiring intensive field instrumentation for an accurate spatial representation. A SVAT model driven by observed meteorological forcing and land surface data can help into understanding these processes. Figure 2 presents the spatial distribution of the available meteorological station over the VAS $50 \times 50\,km^2$ area. An irregular distribution of the stations can be noticed, especially in the center of the area where there is no data. So as to obtain a good representation of soil moisture over the entire area, an interpolation of all the available meteorological stations is necessary. The most adapted method, knowing the number and the localization of the stations, is the inverse distance weighted (IDW) method. Inverse distance weighted methods are based on the assumption that the interpolated surface should be influenced mostly by the nearby points and less by the more distanced points. A

general form of finding an interpolated value u for a given point x is an interpolated function:

$$u(x) = \frac{\sum_{k=0}^{N} w_k(x) u_k}{\sum_{k=0}^{N} w_k(x)} \quad (11)$$

where the weight function is:

$$w_k(x) = \frac{1}{d(x, x_k)} \quad (12)$$

defined by Shepard (1968), x denotes an interpolated (arbitrary point), x_k is the interpolated (known) point , d is a given distance from the known point x_k to the unknown point x and N is the total number of known points. For the interpolation, the $50 \times 50\,km^2$ was divided into 25 areas of $10 \times 10\,km^2$ each. The temperature, atmospheric pressure, wind speed, wind direction, relative humidity were interpolated using just the 4 complete meteorological stations. The shortwave fluxes were extracted from Meteosat while the longwave fluxes were calculated using the formulation from Brutsaert (1975). All 22 stations were taken into account for the precipitation interpolation. Following the interpolation, we have an optimal spatial and temporal distribution of the atmospheric forcing. The data obtained after spatialization thus the aggregated data used in order to simulate the spatialized soil moisture are depicted in Table 3. This allows to simulate the soil moisture over the chosen grid: in this case 25 points. The simple average of all soil moisture data from the 25 areas has been considered as representative for the $50 \times 50\,km^2$. In order to validate this approach, in the next paragraph, a comparison with remote sensing products is presented.

3 Results

So as to quantify the improvement gained from the calibration, an evaluation of the surface soil moisture obtained from ISBA was undertaken.

In a first step the differences when using the default or calibrated version of ISBA are shown by comparing with in situ measurements registered during the MELBEX I campaign. Then, the calibrated version of ISBA was tested by comparing with data from Melbex II campaign. For both cases, the atmospheric forcing used was from Caudete de las Fuentes, a meteorological station located close to the campaigns sites.

In a second step, the calibrated version of ISBA as well as the spatialization method described in the previous section was used so as to have a spatial distribution of soil moisture over the entire catchment. The accuracy of the method was tested and the next paragraph presents a comparison between the spatialized soil moisture and remotely sensed data. As the area was divided into 25 pixels ($10\times10\,km^2$ each), in order to have a representative value over the entire $50\times50\,km^2$, obtained data were averaged both spatially and over time. The soil moisture simulations were extracted for the time steps close to the overpass times of the satellites. The penetration depth was also considered.

3.1 Results at local scale

3.1.1 Calibration of the ISBA model using Melbex I campaign

Figure 3 compares the soil moisture from the Melbex I campaign and the soil moisture simulated with ISBA using the parametrization described in Sect. 2.3 (default and the new set of equations). The precipitation recorded at the meteorological station Caudete de las Fuentes are represented in blue. The simulations were done for the period 2004–2007. For graphical convenience, only the period corresponding to Melbex I campaign (14 July–31 December 2005) is presented.

Using the initial equations, the model tended to overestimate soil moisture in the dry season (from July to September) and to underestimate soil moisture for the rest of the period. In general we can observe a good agreement between the two datasets R^2=0.7934, but the RMSE value equal to 0.0418 m^3/m^3 was higher than the SMOS requirements $-0.04\,m^3/m^3$. In order to minimize this error, the SVAT model was cali-

brated (see Sect. 2.3). Table 4 presents the calculated soil hydraulic values using the default equations and the calibrated ones (Table 2).

Using the default equations (see Table 2), the SVAT model was not able to represent faithfully the dynamics of the first layer of soil during the dry season, keeping it at high soil moisture values (more than $0.10\,m^3/m^3$). In order to enable lower values of soil moisture into the dry season, the wilting point equation was modified as follows. The value obtained for the wilting point using the default equation is about $0.14\,m^3/m^3$, whereas the minimum observed value of soil moisture during the campaign was $0.04\,m^3/m^3$. This behavior was also observed by Pellarin et al. (2009), where a value of wilting point of $0.04\,m^3/m^3$ was used for the simulation in Niger. The default equation was modified so as to retrieve a more representative value to simulate the dry period. The obtained value for the wilting point using the calibrated equation (see Table 2) is $0.0664\,m^3/m^3$. In addition, the default equation for volumetric water content at saturation (w_{sat}) was also optimized. The simulated soil moisture value using the default ISBA was not able to reach the maximum values of soil moisture recorded during the campaign. A value of about $0.5\,m^3/m^3$, obtained using the calibrated equation, seems more representative of a sandy soil (47% sand, 38% silt and 15% clay) at least for the first centimeters of soil.

The simulated soil moisture is driven mostly by the weather patterns and especially by the precipitation. The temporal behavior of surface soil moisture has a saw tooth trend: sharp increase and exponential decline which are caused, respectively by rainfall events and consecutive drying periods. By increasing the coefficient of the retention curve and reducing the hydraulic conductivity at saturation by the use of the calibrated equations, the drainage dynamics were slowed down in order to encounter the same behavior as for the measured soil moisture. The equation for the computation of field capacity was not changed after optimization. The matric potential at saturation has no important effects on the soil moisture modelling so the formulation for the computation of this parameter was only slightly modified in the optimization process.

Using the calibrated version of ISBA a significant improvement (see Table 5) was

obtained for the modelled soil moisture at the first 5 cm (R^2=0.9074). A good quantitative agreement is found (RMSE=0.0220 m^3/m^3) between the two soil moisture data: the same variability, the same drying slope, same low levels and amplitudes. At the beginning of November a higher level of modelled surface soil moisture dynamics is observed compared with in situ data. This can be due to the high value of w_{sat} but can also be due to the differences between the weather patterns between the two places (almost 1.5 km distance between the localization of the meteorological station Caudete de las Fuentes and the place where the Melbex I campaign took place).

3.1.2 Validation of ISBA new parametrization using Melbex II campaign

The first step into our study was to find a parametrization of the surface model which minimizes the error compared with in situ measurements. In order to evaluate the validity of the chosen optimization, the same equations (see Table 2) as described in Sect. 2.3 were used for Melbex II area. Figure 4 presents a comparison between Melbex II data (in black) and simulated soil moisture (in red). A good agreement is retrieved between the two soil moisture data RMSE=0.0240, R^2=0.9096. Some differences can be observed on 10 August and also on 15 September. These differences can be mostly associated to the fact that the meteorological station used is situated at almost 1.5 km from the place were the campaign took place. The precipitations can be slightly different from what occurred at the experimental site.

3.2 Comparison with remote sensing data

3.2.1 Comparison with AMSR-E data

The next step is to check the validity of the approach using satellite data. In this context, a comparison between spatialized soil moisture and the AMSR-E soil moisture product (Njoku L3) was done. The simulated soil moisture as well as the AMSR-E soil moisture product used are representative for the 50×50 km^2 area. The penetration depth of

AMSR-E sensor is considered to be at about 2 cm so the soil moisture for the first two simulated layers was considered. The comparison was done for 2005 to 2007. In this article, due to the fact that the same evolution was observed, only the 2005 period was considered. In a first step, the absolute values of the AMSR-E soil moisture product were compared with the simulated spatialized data. A severe lack of soil moisture dynamics and also a big difference between the absolute value of the two set of data is observed (RMSE=0.0618, MBIAS=0.0121, R^2=0.0439). Because of the different soil moisture dynamics and biases, it is difficult to compare the various datasets in detail. Consequently, all next comparison will be undertaken with normalized data, leading to the lose of the absolute aspects.

The results of this normalization can be seen in Fig. 5. The dynamics of the soil moisture are very well captured at the beginning and also at the end of the year, from January to March we observed an RMSE=0.17, R^2=0.47 and at the end of the year, from October to December RMSE=0.15, R^2=0.43. In the winter season the signal of AMSR-E soil moisture shows a small difference compared with the spatialized soil moisture. This may be explained by the sensitivity of the microwave signal to soil freezing and by the reduced dynamics of the surface soil moisture during winter. In the middle of the year, from April to September, the opposite trend is observed between both datasets. From April to September no correlation is observed (R^2=0.15) and the RMSE is twice than the rest of the year (0.4011).

The inversion algorithm for the AMSR-E soil moisture uses the 10.7 GHz and 18.7 GHz brightness temperature data (Njoku et al., 2003). The increased attenuation by vegetation and the superficial sensing depth (on the order of 1 cm for bare soil) for higher frequencies is a limit in the soil moisture retrieval from AMSR-E data. At this frequency the vegetation has an important influence on the measured signal. This can be seen by plotting the leaf area index (Modis) corresponding to the site. When the growing season begins, the AMSR-E signal is very perturbed.

The polarization ratio provides a better agreement (than the soil moisture product from AMSR-E) with simulated soil moisture even in the vegetation growing period. This

is demonstrated by the increasing statistics: at the beginning of the year, from January to March we observed an RMSE=0.1188, R^2=0.6733, at the end of the year, from October to December RMSE=0.13, R^2=0.63 and in the middle of the year, from April to September R^2=0.4757 and the RMSE=0.1562. It shows that its dynamics is well correlated to the soil moisture variations.

3.2.2 Comparison with ERS-SCAT data

A comparison was also performed between spatialized soil moisture and the ERS-SCAT soil moisture product (Wagner SSM). The derived soil moisture product represents the content of the first cm of the soil in relative units between totally dry conditions (0%) and total water capacity (100%). The spatial resolution is of 50 km with a grid spacing of 12.5 km so over the VAS area we have 16 pixels. In order to have a maximum temporal and spatial cover, the mean of the 16 pixels was used to be compared with simulated data.

In order to compare the two sets of data, the absolute values of the simulated soil moisture were normalized between [0, 1]. The penetration depth of ERS-SCAT sensor is considered to be at about 2 cm so the mean of the first two simulated layers from ISBA was considered. Figure 6 presents the comparison between simulated and observed surface soil moisture during 1 year period. At the beginning of the year, from January to March RMSE=0.2076, R^2=0.0661 and at the end of the year, from October to December RMSE=0.28, R^2=0.0178. An underestimation of the soil moisture level by the ERS-SCAT product is observed. In the middle of the year, from April to September (R^2=0.0427, RMSE=0.19), as for the AMSR-E soil moisture product, the vegetation influence the ERS-SCAT signal. This leads to an overestimation of the soil moisture estimates during the vegetation growing period.

For 2005 only 45 observations were available over the 50×50 km^2 area. A frequent revisit time is important for hydrologic applications, especially to obtain adequate sampling of surface wetting and drying between precipitation events.

4 Conclusions

In the framework of ESA's Soil Moisture and Ocean Salinity mission, this paper investigates the ability to produce simulated soil moisture maps at SMOS pixel scale by using ISBA model. The study has been performed for 2005–2007 over the Valencia Anchor Station, which was selected to be one of the main key test site for the SMOS Calibration/Validation activities. Based on local atmospheric and surface observations from Valencia Anchor Station, it was found that calibrated ISBA model was able to faithfully model the hydrological processes at the surface level. A new databases for soil hydraulic parameters was established so as to improve the soil moisture simulations. By optimizing parameters such as the wilting point (w_{wilt}), hydraulic conductivity at saturation (k_{sat}), saturated soil moisture (w_{sat}), the coefficient of the water retention curve (b) or the matric potential at saturation (Ψ_{sat}) the results obtained by comparing with in situ measurements are significantly improved: the RMSE decrease from 0.0418 m^3/m^3 when using the default ISBA to 0.0220 m^3/m^3 using the calibrated version. The new parametrization was validated by the use of other dataset of soil moisture ground measurements. The value of 0.0240 m^3/m^3 obtained for the RMSE is perfectly adequate for assessing the SMOS validation with an accuracy better than 0.04 m^3/m^3.

Knowing accurately the spatial distribution of soil moisture at large scales is a difficult task requiring intensive field measurements. So as to have a spatial distribution of the soil moisture over the $50 \times 50\,km^2$ area, a spatialization of atmospheric forcing has been done. In order to test the accuracy of this method, a comparison between the simulated spatialized soil moisture and remotely sensed data was performed. Data from two sensors were used: AMSR-E and ERS-Scat. The soil moisture simulations were extracted for the time steps close to the overpass times of the satellites. The penetration depth and the re-sampling grid of the soil moisture products used for each satellite was also considered.

Although AMSR-E surface soil moisture product is not able to capture the absolute value, it provides reliable information on surface soil moisture temporal variability, at

seasonal and rainy events scale. In the middle of the year, from April to September, the vegetation has an important influence on the measured signal. During the growing season the AMSR-E signal is very perturbed. The polarization ratio 6.9 GHz provides a better agreement with simulated soil moisture even in the vegetation growing period.

A comparison was done between spatialized soil moisture and the ERS-SCAT soil moisture product (Wagner SSM). In this case also the seasons are well marked but the lack of a higher temporal resolution (45 observations were available over the area for 2005) of soil moisture data over the area is a limit.

This study presents the required first step procedure necessary to provide soil moisture mapping over a large scale. This is important to acquire a soil moisture data base at SMOS scale. As the soil moisture simulation process is now validated, future works will be devoted to obtain accurate brightness temperature maps to be compared with real SMOS data. This work is essential in the validation process of the SMOS mission.

Acknowledgements. The authors wish to thank the European Space Agency (ESA), the Centre National d'Etudes Spatiales (CNES), the Centre National de la Recherche Scientifique – Institut National des Sciences de l'Univers (CNRS- INSU SIC) and the French National Programme TOSCA (Terre, Océans, Surfaces Continentales et Atmosphère) for supporting this work. We also wish to thank the NASA National Snow and Ice Data Center (NSIDC) for providing AMSR-E data as well as the Institute for Photogrammetry and Remote Sensing, Vienna University of Technology, Vienna, Austria for providing the ERS-Scat data. We thank also the Centre national de Recherches Météorologiques and Jean Christophe Calvet (CNRM) - Météo-France for the SURFEX model.

cnrs INSU
Institut national des sciences de l'Univers

The publication of this article is financed by CNRS-INSU.

References

Betts, A., Ball, J., Beljaars, A., Miller, M., and Viterbo, P.: The land surface-atmosphere interaction : A review based on observational and global modeling perspectives, J. Geophys. Res., 101(D3), 7209–7225, 1996. 651

Boone, A.: Modelisation des processus hydrologiques dans le schema de surface ISBA: Inclusion d'un reservoir hydrologique, du gel et modelisation de la neige., PhD thesis, University Paul Sabatier, Toulouse, France, 252 pp., 2000. 659

Boone, A., Calvet, J.-C., and Noilhan, J.: The inclusion of a third soil layer in a Land Surface Scheme using the Force-Restore method., J. Appl. Meteorol., 38, 1611–1630, 1999. 659, 662, 677

Boone, A., Masson, V., Meyers, T., and Noilhan, J.: The influence of the inclusion of soil freezing on simulations by a soil-vegetation-atmosphere transfer scheme., J. Appl. Meteorol., 39, 1544–1569, 2000. 659

Bosch, D. D., Lakshmi, V., Jackson, T. J., Choi, M., and Jacobs, J. M.: Large scale measurements of soil moisture for validation of remotely sensed data: Georgia soil moisture experiment of 2003, J. Hydrol., 323, 120–137, 2006. 651

Braud, I., Noilhan, J., Bessemoulin, P., Mascart, P., Havercamp, R., and Vauclin, M.: Bare-ground surface heat and water exchanges under dry conditions: Observations and parameterization., Bound.-Lay. Meteorol., 66, 173–200, 1993. 660

Brooks, R. H. and Corey, A. T.: Properties of porous media affecting fluid flow, J. Irrig. Drain. American Soc. Civil Eng., IR 2, 61–88, 1966. 660

Brutsaert, W. H.: On a derivable formula for long-wave radiation from clear skies, Water Resour. Res., 11(2), 742–744, 1975. 663

Calvet, J.-C., Noilhan, J., and Bessemoulin, P.: Retriving the root-zone soil moisture from surface soil moisture or temperature estimates : a feasibility study based on field measurements., J. Appl. Meteorol., 37, 371–386, 1998. 658

Cano, A., Millan-Scheiding, C., Wigneron, J.-P., Antolin, C., Balling, J., Grant, J., Kruszewski, A., Saleh, K., Sobjaerg, S., Skou, N., and Lopez-Baeza, E.: The Mediterranean Ecosystem L-Band EXperiment over vineyards (MELBEX-II)., 10th Specialist Meeting on Microwave Radiometry and Remote Sensing for the Environment, Italy, 2008. 655

Cano, A., Saleh, K., Wigneron, J. P., Antolín, C., Balling, J., Kerr, Y. H., Kruszewski, A., Millán-Scheiding, C., Søbjaerg, S. S., Skou, N., and López-Baeza, E.: The SMOS Medierranean

Ecosystem L-band experiment (MELBEX-I) over natural shrubs, Remote Sensing of Environment, http://dx.doi.org/10.1016/j.rse.2009.11.019, doi:10.1016/j.rse.2009.11.019, 2009. 654
Clapp, R. B. and Hornberger, G. M.: Empirical Equation for some soil hydraulic properties, Water Resour. Res., 14, 601–604, 1978. 660
Cosby, B. J., Hornberger, G. M., Clapp, R. B., and Ginn, T. R.: A Statistical exploration of the relationships of soil moisture characteristics to the physical properties of soils, Water Resour. Res., 20, 682–690, 1984. 662, 677
Delwart, S., Bouzinac, C., and P., W.: Overall SMOS Cal/Val Plan and Requirements, SMOS 7th WORKSHOP, ESRIN, 2007. 652
Entekhabi, D. and Rodrigues-Iturbe, I.: An analytic framework for the characterization of the space-time variability of soil moisture., Adv. Water Res., 17 (1-2), 35–45, 1994. 651
Entekhabi, D., Rodrigues-IturbeNakamura, I., and Castelli, F.: Mutual Interaction of Soil Moisture state and atmospheric processes., J. Hydrol., 183, 3–17, 1996. 651
Giordani, H., Expériences de validation unidimensionnelles du schéma de surface NP89 aux normes Arpge sur trois sites de la campagne EFEDA 91, Note de travail 24 GMME/Météo-France, 1993 662, 677
Gruhier, C., de Rosnay, P., Kerr, Y. H., Mougin, E., Ceschia, E., Calvet, J.-C., and Richaume, P.: Evaluation of AMSR-E soil moisture product based on ground measurements over temperate and semi-arid regions, Geophys. Res. Lett., 35, L10405, doi:10.1029/2008GL0333330, 2008. 656
Jackson, T. J., LeVine, D., Swift, C., Schmugge, T. J., and Schiebe, F.: Large area mapping of soil moisture using the ESTAR passive microwave radiometer., Remote Sens. Environ., 54(1), 27–37, 1995. 652
Jackson, T. J., Le Vine, D. M., Hsu, A., Oldack, A., Starks, P., Swift, C., Isham, J., and Haken, M.: Soil moisture Mapping at regional scales using microwave radiometry: The southern great plains hydrology experiment, IEEE Trans. Geosc. Remote Sens., 37(5), 2136–2151, 1999. 652
Jones, A., Vukićević, T., and Vonder Haar, T.: A microwave satellite observational operator for variational data assimilation of soil moisture, J. Hydrometeorol., 5, 213–229, 2004. 651
Kerr, Y. H.: Soil Moisture from space: Where we are ?, Hydrogeol. J., 15, 117–120, 2007. 651
Kerr, Y. H., Waldteufel, P., Wigneron, J.-P., Martinuzzi, J.-M., Font, J., and Berger, M.: Soil moisture retrieval from Space: The soil moisture and ocean salinity (SMOS) mission, IEEE Trans. Geosc. Remote Sens., 39 (8), 1729–1735, 2001. 651, 652

Le Moigne, P., Boone, A., Calvet, J.-C., Decharme, B., Faroux, S., Gibelin, A.-L., Lebeaupin, C., Mahfouf, J.-F., Martin, E., Masson, V., Mironov, D., Noilhan, J., Tulet, P., and Van Den Hurk, B.: SURFEX scientific documentation, 2009. 658

Lopez-Baeza, E., Antolín Tomás, C., Bodas Salcedo, A., Gimeno Ferrer, J. F., Saleh Contell, K., Ferrer, F., Castell Balaguer, N., Doménech García, C., Sanchez Alandí, M. A., and Velázquez Blázquez, A.: The Valencia Anchor Station: A Reference Cal/Val Area for Low-Resolution Remote Sensing Data and Products., Recent Advances in Quantitative Remote Sensing, Torrente (Valencia) – poster, 2002. 653

Lopez-Baeza, E., Alonso, S., Comerón, A., Diaz-Pabon, R., Domenech, C., Gimeno-Ferrer, J., Jorge, J., Labajo, A., Pineda, N., Pino, D., Rius, A., Rocadenbosch, F., Saleh, K., Sicard, M., Tarruella, R., Torrobella, J., and Velazquez, A.: A High-Quality Dataset of Land-Surface and Atmospheric Measurements for the Comparison/Crosscalibration of Data From Large Scale Optical Earth Observation Sensors in Space. The Valencia Anchor Station, Proceedings of the Workshop on Inter-Comparison of Large Scale Optical and Infrared Sensors, ESA/ESTEC 12–14 October 2004, ESA-WPP-244, 2005a. 652

Lopez-Baeza, E., Alonso, S., Comerón, A., Diaz-Pabon, R., Domenech, C., Gimeno-Ferrer, J. F., Jorge, J., Labajo, A. , Pineda, N., Pino, D., Rius, A., Rocadenbosch, F., Saleh, K., Sicard, M. , Tarruella, R. Torrobella, J., and Velazquez, A.: Proposal of a Water Cycle Observatory: The Reference Valencia and Alacant Anchor Stations for Remote Sensing Data and Products, XI Spanish Remote Sensing Congress, Puerto de la Cruz, Tenerife, 2005. 652

Lopez-Baeza, E., SVRC, and team: Validation of SMOS Products over Mediterranean Ecosystem Vegetation at the Valencia Anchor Station Reference Area, Experimental Plan SMOS Validation Rehearsal Campaign, SMOS Cal/Val AO I.D, 2008. 654

Magagi, R. and Kerr, Y.: Retrieval of soil moisture and vegetation characteristics by use of ERS-1 wind scatterometer over arid and semi-arid areas, J. Hydrol., 188–189, 361–384, 1997. 657

Mahfouf, J.-F. and Noilhan, J.: Comparative study of various formulations of evaporation from bare soil using in situ data, J. Appl. Meteorol., 30, 351–362, 1991. 658

Masson, V., Champeaux, J.-L., Chauvin, F., Meriguet, C., and Lacaze, R.: A global database of land surface parameters at 1-km resolution in meteorological and climate models, J. Climate, 16(9), 1261–1282, 2003. 654

Millan-Scheiding, C., Marco, J., Soriano, M., Torre, E., Torregrosa, G., Abalos, B., Requena, F., Cano, A., Antolin, C., and Lopez-Baeza, E.: VAS Soil and Vegetation Characterization,

SMOS meeting in Bordeaux. INRA, 30–31 October 2008, 2008. 654
Njoku, E. G.: AMSR-E/AQUA daily L3 surface soil moisture, interpretive parms, & QC EASE-Grids, Boulder, CO, USA: National Snow and Ice Data Center, Digital Media, 2004. 656
Njoku, E. G. and Entekhabi, D.: Passive microwave remote sensing of soil moisture, J. Hydrol., 184, 101–129, 1996. 651
Njoku, E. G., Jackson, T., Lakshmi, V., Chan, T., and Nghiem, S.: Soil moisture retrieval from AMSR-E, IEEE Geosc. Remote Sens. Let., 41(2), 215–229, 2003. 651, 656, 667
Noilhan, J. and Lacarrère, P.: GCM Grid-Scale Evaporation from Mesoscale Modeling, J. Climate., 8, 206–223, 1995. 662, 677
Noilhan, J. and Mahfouf, J.-F.: The ISBA land surface parameterization scheme, Global Planet Change, 13, 145–159, 1996. 652
Noilhan, J. and Planton, S.: A simple parameterization of land surface fluxes processes for meteorological models, Mon. Weather. Rev., 117, 536–549, 1989. 652, 658
Pellarin, T., Laurent, J., Cappelaere, B., Decharme, B., Descroix, L., and Ramier, D.: Hydrological modelling and associated microwave emission of a semi-arid region in South-western Niger, J. Hydrol., J. Hydrol., 2009, 375 (1–2), 262–272, doi:10.1016/j.jhydrol.2008.12.003, 2009. 665
Rüdiger, C., Calvet, J.-C., Gruhier, C., Holmes, T. R. H., de Jeu, R. A. M., and Wagner, W.: An Intercomparison of ERS-Scat and AMSR-E Soil Moisture Observations with Model Simulations over France, American Meteorological Society, 10, 431–447, 2009. 656
Schmugge, T., Jackson, T., Kustas, T. J., and Schmugge, T., Jackson, T., Kustas, T. J., and Wang, J. R. : Passive microwave remote sensing of soil moisture: results from HAPEX, FIFE and MONSOON'90, ISPRS J. Photogramm., 47, 127–143, 1992. 652
Shao, Y. and Henderson-Sellers, A.: Validation of soil moisture simulation in land surface parameterisation schemes with HAPEX data, Global Planet. Change, 13, 11–46, 1996. 661
Shepard, D.: A two-dimensional interpolation function for irregularly-spaced data, Proceedings of the 1968 ACM National Conference, p. 517524, 1968. 663
Wagner, W., Lemoine, G., and Rott, H.: A Method for Estimating Soil Moisture from ERS Scatterometer and Soil Data, IEEE Trans. Geosc. Remote Sens., 70(2), 191–207, 1999a. 651, 657
Wagner, W., Noll, J., Borgeaud, M., and Rott, H.: Monitoring soil moisture over the Canadian prairies with the ERS scatterometer, IEEE Trans. Geosc. Remote Sens., 37, 206–216, 1999b. 657

Wagner, W., Blöschl, G., Pampaloni, P., Calvet, J.-C., Bizzarri, B., Wigneron, J.-P., and Kerr, Y.: Operational readiness of microwave remote sensing of soil moisture for hydrologic applications, Nord. Hydrol., 38(1), 1–20, 2006. 651

Wang, J. R., Shiue, J. C., Schmugge, T. J. and Engman, E. T.: The L-band PBMR measurements of surface soil moisture in FIFE, IEEE Trans. Geosc. Remote Sens., 28, 906–914, 1990a. 652

Wigneron, J.-P., Calvet, J.-C., Pellarin, T., Van de Gried, A., Berger, M., and Ferrazzoli, P.: Retrieving near-surface soil moisture from microwave radiometric observations: current status and future plans, rse, 85(4), 489–506, 2003.

651

Table 1. Coordinates of the meteorological stations located into the 50×50 km^2 area.

Station Name	Longitude	Latitude	Characteristics
VAS	1.288° W	39.571° N	Fully equipped station
CASAS DE VES	1.330° W	39.262° N	Rain gauge
CASAS IBANEZ	1.465° W	39.288° N	Rain gauge
VILLAMALEA	1.598° W	39.363° N	Rain gauge
REQUENA LA PORTERA COOP.	1.101° W	39.405° N	Rain gauge
REQUENA CAMPO ARCIS	1.165° W	39.436° N	Rain gauge
DEL MORO C H JUCAR	1.355° W	39.484° N	Rain gauge
REQUENA	1.096° W	39.484° N	Rain gauge
CAUDETE DE LAS FUENTES	1.317° W	39.523° N	Rain gauge
MINGLANILLA	1.595° W	39.538° N	Rain gauge
PRESA DE CONTRERAS	1.505° W	39.542° N	Rain gauge
UTIEL C.H. JUCAR	1.206° W	39.568° N	Rain gauge
UTIEL	1.205° W	39.575° N	Rain gauge
UTIEL (LA CUBERA – AUTOMATICA)	1.249° W	39.580° N	Fully equipped station
CAMPORROBLES COOPERATIVA	1.402° W	39.649° N	Rain gauge
CAMPO ARCIS	1.168° W	39.433° N	Fully equipped station
CERRITO REQUENA	1.107° W	39.480° N	Fully equipped station
GRAJA DE INIESTA	1.674° W	39.516° N	Rain gauge
CONTRERAS	1.498° W	39.540° N	Rain gauge
CAUDETE DE LAS FUENTES I	1.280° W	39.547° N	Rain gauge
VILLAMALEA I	1.602° W	39.365° N	Rain gauge
CERRO	1.512° W	39.259° N	Rain gauge

Table 2. Equation of hydrological parameters used in default (DEFAULT ISBA (1) see Giordani, 1993; Noilhan and Lacarrère, 1995) and calibrated (CALIBRATED ISBA (2) see Cosby et al. (1984) and Boone et al., 1999) version of ISBA.

VARIABLE	DEFAULT ISBA (1)	CALIBRATED ISBA (2)
b	b=13.7*CLAY+ 3.501	b_mean=3.10+0.157*CLAY*100+(−0.003)*SAND*100 b_st_dev = 0.92+0.049*CLAY*100+(100−CLAY*100−SAND*100)*0.014 b=b_mean+b_st_dev
Ψ_{sat} (m)	$\Psi_{sat}=-10^{(1.85-0.88*SAND)}*0.01$	Ψ_{sat_mean} =(1.54+(−0.010)*SAND*100+0.006*(100−CLAY*100−SAND*100)) $\Psi_{sat\_st\_dev}$ =(0.72+(−0.0026)*(100−CLAY*100−SAND*100)+0.001*CLAY*100) $\Psi_{sat} = -(10^{\Psi_{sat\_mean}-\Psi_{sat\_st\_dev}}/100)$
k_{sat}(mm^{-1})	k_{sat}=see (*)	k_{sat_mean} = (-0.60+0.013*SAND*100+(-0.0064)*CLAY*100) $k_{sat\_st\_dev}$ = (0.43+0.003*(100−CLAY*100−SAND*100)+0.001*CLAY*100) $k_{sat} = 10^{k_{sat\_mean}-k_{sat\_st\_dev}} * (2.54/360000)$
w_{sat}(m^{3}m^{-3})	w_{sat}=0.001* (−108*SAND+494.305)	$w_{sat\_mean} = (50.5 + (-0.142) * SAND * 100 + (-0.037) * CLAY * 100)/100$ $w_{sat\_st\_dev}$=(8.23+(−0.081)*CLAY*100+(−0.007)*SAND*100)/100 $w_{1sat} = w_{sat\_mean} + w_{sat\_st\_dev}$
w_{wilt} (m^{3}m^{-3})	w_{wilt}=37.134 E−3*CLAY$^{0.5}$	w_{wilt} = 17.134 E−3*CLAY$^{0.5}$
w_{fc}(m^{3}m^{-3})	w_{fc}=89.047 E−3*CLAY$^{0.349}$	w_{fc}=89.047 E−3*CLAY$^{0.349}$

*: 1.0e−6*10 (0.162E+01−0.582E+01*CLAY −0.907E−01*SAND+0.529E+01*CLAY^2+0.120E+01*SAND^2)

HESSD
7, 649–686, 2010

Table 3. Resolution and data used as input of the SVAT model in order to obtain the spatialized soil moisture.

VARIABLE	INPUT sources	OUTPUT resolution
LAI	MODIS – 1 km resolution	aggregated to 10×10 km^2
ROUGHNESS	ECOCLIMAP – 1 km resolution	aggregated to 10×10 km^2
FRACTION OF VEGETATION	ECOCLIMAP – 1 km resolution	aggregated to 10×10 km^2
TEXTURE	clay and sand map at 10 m resolution	aggregated to 10×10 km^2
TEMPERATURE	4 meteorological stations	interpolated at 10×10 km^2
PRESSURE	4 meteorological stations	interpolated at 10×10 km^2
WIND SPEED	4 meteorological stations	interpolated at 10×10 km^2
WIND DIRECTION	4 meteorological stations	interpolated at 10×10 km^2
RELATIVE HUMIDITY	4 meteorological stations	interpolated at 10×10 km^2
SHORTWAVE fluxes	METEOSAT	extracted at 10×10 km^2
LONGWAVE fluxes	calculated using interpolated atmospheric data	
PRECIPITATION	22 meteorological stations	interpolated at 10×10 km^2

Table 4. Soil hydraulic values for MELBEX I site calculated using the default and the calibrated set of equations.

	b	Ψ_{sat} (m)	k_{sat} (m m^{-1})	w_{sat} (m^3 m^{-3})	w_{wilt} (m^3 m^{-3})	w_{fc}(m^3 m^{-3})
DEFAULT ISBA	5.556	−0.172	1.225E-05	0.444	0.144	0.230
CALIBRATED ISBA	7.519	−0.049	1.502E-06	0.499	0.066	0.230

Table 5. Statistics obtained by comparing the in situ measurements from MELBEX I campaign with the default/calibrated simulated soil moisture using ISBA.

	R^2	RMSE	MEAN BIAS
DEFAULT ISBA	0.7934	0.0418	0.0152
CALIBRATED ISBA	0.9074	0.0220	0.0010

HESSD

7, 649–686, 2010

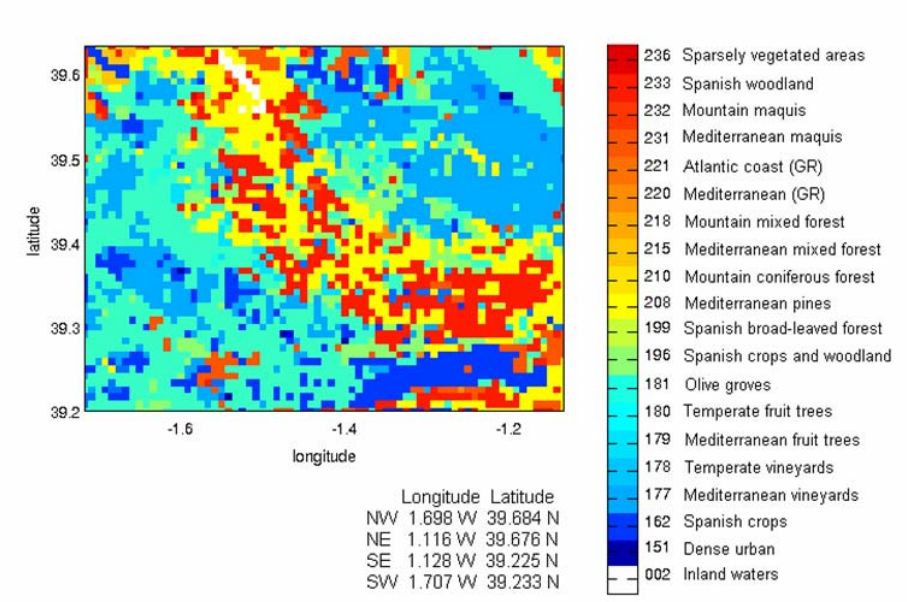

Fig. 1. ECOCLIMAP characteristics over the 50×50 km^2.

HESSD
7, 649–686, 2010

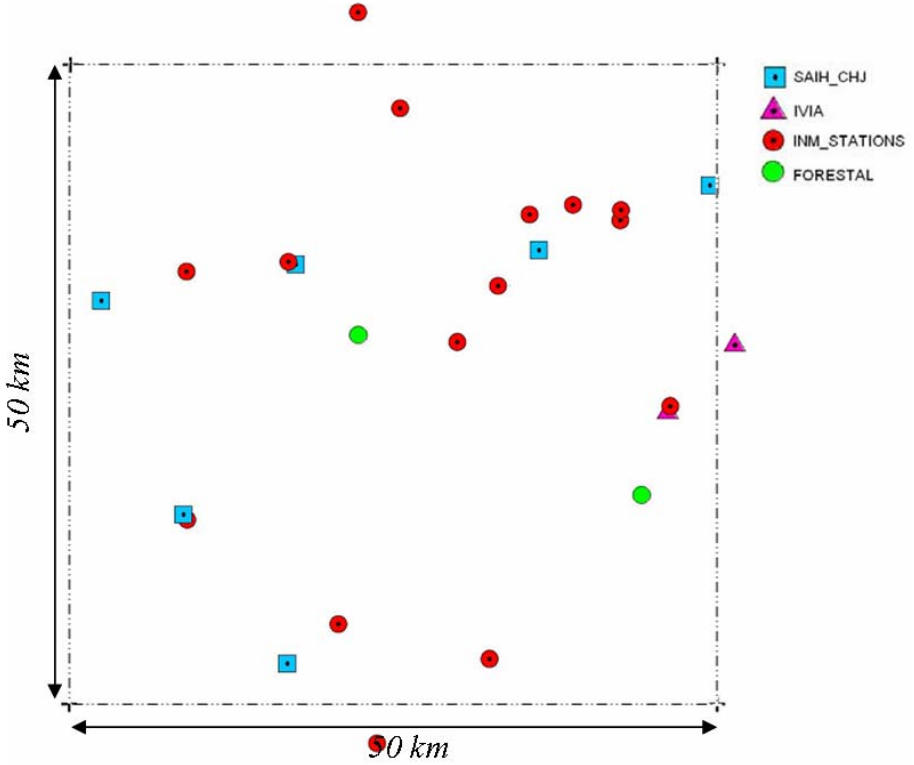

Fig. 2. Distribution of the meteorological stations over the 50×50 km^2 area. SAIH CHJ stands for Sistema Automatica de Informacion Hidrologica Jucar; IVIA stands for Instituto Valenciano de Investigacion Agrarias; INM STATIONS are the meteorological stations from the INSTITUTO NACIONAL de METEOROLOGIA; FORESTAL are the stations own by the forestry authority.

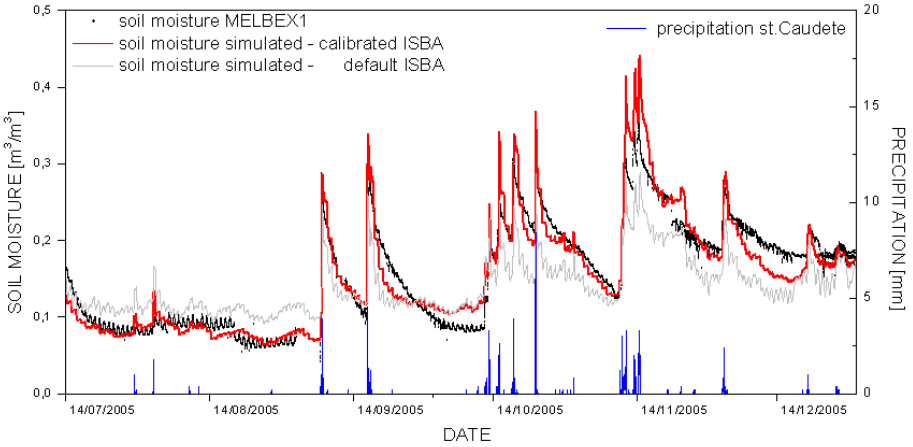

Fig. 3. Comparison between observed (black line) and simulated soil moisture using the default ISBA (clear grey line) and the calibrated ISBA (red line). The precipitation corresponding to the meteorological station Caudete de las Fuentes are represented in blue.

HESSD
7, 649–686, 2010

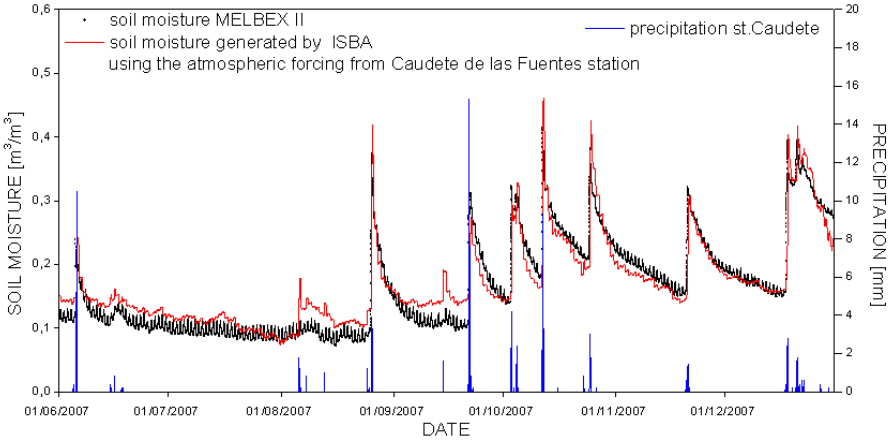

Fig. 4. Comparison between observed (black line) and simulated soil moisture using the calibrated ISBA (red line). The precipitation corresponding to the meteorological station Caudete de las Fuentes are represented in blue.

HESSD
7, 649–686, 2010

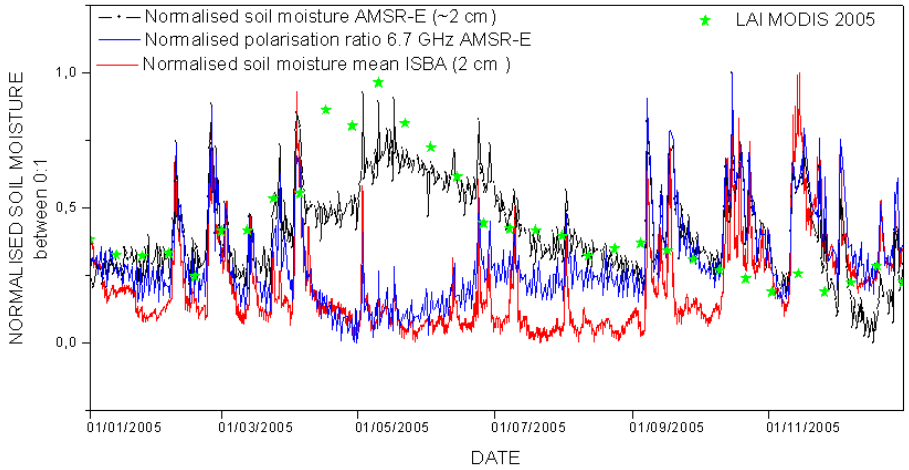

Fig. 5. Comparison between surface soil moisture AMSR-E (black line), spatialized soil moisture from ISBA (red line) and the polarization ratio at 6.9 GHz AMSR-E (blue line). All values are normalized between [0, 1]. The leaf area index from Modis is also represented here (green stars).

HESSD
7, 649–686, 2010

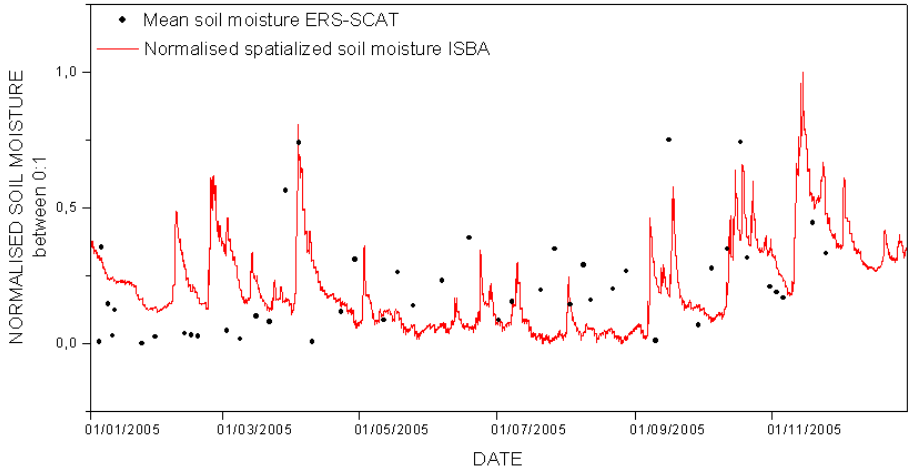

Fig. 6. Comparison between surface soil moisture ERS-SCAT (black stars) and spatialized soil moisture mean from ISBA (red line).

HESSD
7, 649–686, 2010